

Research Paper

Bending of a Homogeneous Beam with a Monosymmetric Cross Section – Shear Effect

Krzysztof MAGNUCKI¹, Ewa MAGNUCKA-BLANDZI²,
Dawid WITKOWSKI¹*, Natalia STEFAŃSKA¹

¹) *Lukasiewicz Research Network – Poznan Institute of Technology*
Poznan, Poland

²) *Institute of Mathematics, Poznan University of Technology*
Poznan, Poland

*Corresponding Author e-mail: dawid.witkowski@pit.lukasiewicz.gov.pl

This paper is devoted to the study of a homogeneous clamped beam with a monosymmetric cross section under uniformly distributed load or three-point bending. A nonlinear shear deformation theory of a plane beam cross section based on the classical shear stress formula known as the Zhuravsky shear stress is developed. The values of shear coefficients and maximum deflections of exemplary beams are analytically determined. Moreover, numerical FEM computations for these beams are carried out. The results of the research from both methods are shown in figures, specified in tables, and compared. The percentage relative differences between the analytical and numerical results prove that the proposed original shear deformation theory accurately describes the shear deformation problem of a beam's planar crosssection.

Keywords: homogeneous beam; nonlinear shear deformation theory; bending; shear effect.

1. INTRODUCTION

Newly designed structures must meet more rigorous criteria resulting from increasingly stringent standards. Engineers are striving to create structures capable of withstanding static, dynamic and thermal loads with greater efficiency while maintaining their strength and enabling weight reduction. The use of modern materials, new ways of structure optimization and development of the theories of solid bodies behavior are becoming essential to meet these requirements.

The shear effect occurring in beams, plates and shells is of significant importance in engineering structures. WANG *et al.* [1] presented the bending, buckling and free vibrations problems of beams and plates, considering the shear

effect theories formulated in past decades. KURRER [2] described the history of structures theory with the detailed list of their authors. The fundamental theories of beam and plate deformation, according to REDDY [3], are based on specific relationships between material properties and nonlinear deformations. These theories include equilibrium equations used to analyze beam deformation and the principle of virtual work, essential in mathematical modeling used in computer simulations and engineering, especially in the finite element method. GAO and SHANG [4], based on loads applied to the upper and lower surfaces of the beam, demonstrated that the overall deformation of beams can be separated into two independent parts: bending and elongation or compression. Without arbitrary assumptions, an accurate theory regarding deep beams, considering these two deformations, is explicitly developed based on the Boussinesq-Galerkin solution and Lure's method. Simultaneously, as a classical example, it is shown that the solution based on this theory is an elastic solution and provides better results than other beam theories.

CARRERA *et al.* [5] discussed various beam theories such as the Euler-Bernoulli theory, Timoshenko theory, and theories involving stretching in the plane. Variants of theories encompassing complete linear extension, Carrera's unified formulation and advanced beam theories based on parabolic, cubic, quartic, and multidimensional assumptions were presented. The paper also focused on potential applications of these theories in analyzing shells and beams made from materials with gradient properties. Additionally, the Arlequin method for creating multi-model beam theories was discussed. CHALLAMEL [6] investigated the buckling of higher-order beam-columns using advanced continuous models. The equivalence between enriched kinematics in traditional higher-order beam theories and the non-local and gradient nature of constitutive laws was demonstrated. This systematized typical beam theories, including the Euler-Bernoulli beam theory, Timoshenko theory, and other higher-order theories. A consistent methodology leading to sensible solutions for buckling-related problems was presented. It was shown that the Timoshenko theory and some other higher-order theories can be understood as non-local or gradient variants of the Euler-Bernoulli beam theory. Furthermore, the problem of higher-order beam-column buckling from the perspective of Timoshenko's gradient elasticity theory was discussed, presenting various models with available solutions for repetitive structures and beams with microstructures.

THAI and VO [7] developed a non-local sinusoidal beam deformation theory to study the bending, buckling, and vibrations of nanobeams. Their model considered both small-scale effects and shear deformations in nanobeams without requiring additional corrective coefficients. Using non-local constitutive relationships by Eringen, authors derived equations of motion and boundary conditions from Hamilton's principle. Analytical solutions for deflection, buckling load, and

natural frequency of simply supported beams were presented and compared with predictions from the non-local Timoshenko beam theory. The results unequivocally confirm the accuracy of this theory in predicting the bending, buckling, and vibrations of short nanobeams where small-scale and shear deformations are significant. In another work by THAI and VO [8], different beam theories for bending and free vibrations of beams with gradient material were investigated, considering a higher degree of shear deformation. These developed theories eliminate the need for a correction factor for shear by considering the variability of deformations on beam surfaces. The similarities of these theories to the Euler-Bernoulli beam theory lie in their equations of motion, boundary conditions, and stresses. The material of the gradient beam assumed a change in properties along the beam according to a power-law distribution of volume fractions. Hamilton's principle was utilized to derive equations of motion and boundary conditions. Analytical solutions obtained were verified by comparison with existing solutions. Finally, the influence of the power-law index and shear deformation on the bending and vibrations of gradient material beams was examined.

AKGÖZ and CIVALEK [9] developed a new beam model considering microstructural effects and shear deformations based on a modified gradient strain theory. This model accurately accounts for these effects without the need for shear corrective coefficients. Hamilton's principle was applied to deduce equations of motion and boundary conditions for freely supported microbeams. The behavior of microbeams under static loads and free vibrations was analyzed. Analytical solutions were obtained for point and uniformly distributed loading deflections and the first three natural frequencies using Navier's solution. Results were compared with other beam theories, both classical and non-classical. Parametric studies showed that the effect of shear deformation becomes more significant for lower slenderness ratios and higher modes of microbeams. REDDY and EL-BORGI [10] developed equations for both Euler-Bernoulli and Timoshenko beams, considering larger rotations than traditional von Kármán strains and material length scales from Eringen's non-local model. They employed the principle of virtual displacements to deduce these equations, taking into account Eringen's non-locality and modified nonlinear von Kármán strains. Subsequently, they created finite element models, presenting numerical results for various boundary conditions and demonstrating the influence of the non-local parameter on beam deflections.

PRADHAN and CHAKRAVERTY [11] investigated the free vibrations of functionally graded (FG) beam materials with different boundary conditions. They used higher-order shear deformation beam theories (SDBTs) to analyze the free vibration response of FG beams. The material properties of FG beams were modeled using a power-law function through the thickness, and test functions describing displacements were expressed algebraically. The Rayleigh-Ritz method

was used to estimate frequencies, accommodating various boundary conditions. Obtained frequencies were compared with literature data, and new results were presented after verifying frequency convergence. It is worth mentioning that higher-order shear deformation theory can be used to obtain very precise solutions for beams and plates problems. This issue is discussed by MALIKAN and EREMEYEV [20]. The paper takes into account the disadvantage of the material composition of thick beams made of functionally graded materials (FGM). Beam model consists of a novel shear stress strain distribution shape function in the transverse coordinate. Beam theory also takes into account the stretching effect to represent the indirect effect of thickness changes. SENJANOVIĆ *et al.* [12] presented a consistent theory of first-order shear deformation plates, utilizing Hamilton's principle. The governing equation for shear deformation is a sixth-order partial differential equation in both the x and y axes. Additionally, an advanced theory providing force equilibrium based on bending deformation was presented as a fourth-order equation. Analytical solutions for specific cases are presented, and natural frequencies are compared with those obtained using Rayleigh-Ritz methods within Mindlin's classical thick plate theory. The study includes an evaluation of the reliability of these two first-order shear deformation plate theories.

ÖZÜTOK and MADENCI [13] developed mixed finite element method (MFEM) equations for composite laminated beams using functionals derived from the Gâteaux differential (GD) approach. They proposed a higher-order shear deformation theory (HOBT) considering nonlinear distributions of shear stresses throughout the thickness of the laminated beam. Field equations for such beams were derived from the principle of virtual displacements. Subsequently, using mathematical methods, they obtained functionals with boundary conditions employing the GD method. Based on this, the HOBT10 beam element with 10 degrees of freedom, encompassing displacements, rotations, higher-order bending moments, and shear forces, was developed. A comparison was made with Euler-Bernoulli beam theory and first-order shear deformation theory to better understand the results of static analysis of composite layered beams. The efficiency of the element was verified by applying it to several test problems. FAGHIDIAN [14] employed Reissner's mixed variational principle to formulate dynamic equilibrium conditions, considering nonlinear bending of beams with actual shear stresses. A nonlinear nano-Reissner beam model was developed based on Eringen's non-local gradient elasticity theory. An analysis of nonlinear deflections was conducted and compared to results from the size-dependent Timoshenko's beam theory. The differences between Timoshenko's beam theory and Reissner's model were discussed in detail. It was demonstrated that the Reissner beam model is not a first-order shear deformation theory, as it considers the influence of actual shear and normal stresses. Furthermore, both

linear and nonlinear deflections according to the Reissner beam theory were consistently lower than those predicted by the Timoshenko theory for different gradient elasticity theories.

The development of shear deformation theories in beams and plates was presented in the work by CHALLAMEL and ELISHAKOFF [15]. LIN *et al.* [16] analyzed vibrations and buckling of nanobeams, considering surface stress effects. A material model was presented, where the core of the beam is a single-crystal material with specific crystallographic directions, and the beams covered with atomic layers having the same crystallographic directions on both surfaces. The general third-order theory of higher-order shear deformation was used to derive the total energy functional of the beam. By minimizing this functional using the p -Ritz method, eigenvalue equations describing buckling and vibrations of nanobeams were obtained, considering surface stress effects. The behavior of beams was thoroughly analyzed, comparing them with first-order theories and Reddy's third-order theory, showing that both theories might inaccurately capture the influence of surface stresses on nanobeam behavior. It was indicated that surface stress effects on buckling and vibrations of nanobeams made from single-crystal nickel exhibit a different trend compared to first-order theory or Reddy's third-order theory.

MAGNUCKI *et al.* [17] tackled the topic of nanobeams, specifically analyzing vibrations and buckling of nanobeams considering surface stress effects. A beam model was presented, where the core takes the form of a single-crystal material with defined crystallographic directions. The beams are coated with atomic layers having identical crystallographic directions on both the upper and lower surfaces. An advanced third-order theory of shear deformation was used to obtain the total energy functional of the beam. By minimizing this functional using the p -Ritz method, eigenvalue equations describing buckling and vibrations of nanobeams, considering surface stress effects, were obtained. A detailed analysis was conducted, comparing the buckling and vibrations with the results obtained from first-order theory and Reddy's third-order theory. It was found that in certain cases, both first-order and Reddy's third-order theories might inaccurately describe the influence of surface stresses on nanobeam vibrations and buckling. The effects of surface stresses on buckling and vibrations of nanobeams made from single-crystal nickel, obtained using the advanced third-order theory, showed a contrary trend compared to the results obtained from first-order theory or Reddy's third-order theory. A folded beam model subjected to force at three points was developed analytically based on the assumption of a piecewise-linear profile [18]. Similar to [24], homogeneous beams with two-sided symmetric cross-sections, sandwich beams, and beams with variable mechanical properties in the depth direction are investigated. By considering the minimization of energy principle, two differential equilibrium equations are obtained [19]. The

system of equations is solved analytically, and shear coefficients and beam deflections are obtained. Additionally, stress patterns for selected cross-sections are determined and compared with stresses determined using Zhuravsky's formula [21]. Subsequently, a theory of cross-sectional shear deformation for flat beam is formulated [22]. Similarly to work [23], the bending problem of these beams was also numerically examined using the finite element method.

2. ANALYTICAL MODEL OF THE HOMOGENEOUS BEAM WITH MONOSYMMETRIC CROSS SECTION

The homogeneous beam of length L with clamped ends is subjected to three-point bending (Fig. 1). The beam is situated in the Cartesian coordinate xyz .

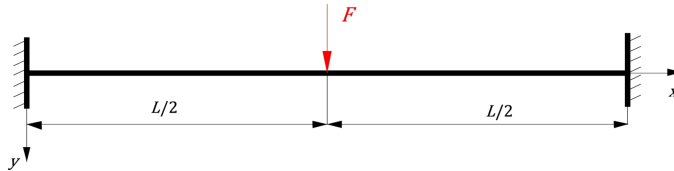


FIG. 1. Scheme of the homogeneous beam with clamped ends.

The beam cross section of depth h is shown in Fig. 2.

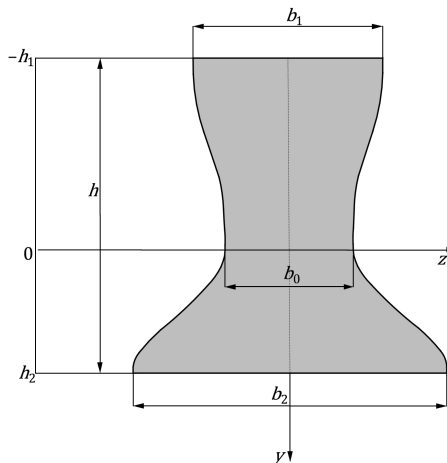


FIG. 2. Scheme of the monosymmetric cross section of the beam.

The symmetrical variation of the cross section width in the depth direction is as follows:

- for the upper part ($-\chi_1 \leq \eta \leq 0$):

$$(2.1) \quad \begin{aligned} b^{(1)}(\eta) &= b_0 \bar{b}^{(1)}(\eta), \\ \bar{b}^{(1)}(\eta) &= 1 + \frac{1}{2} \beta_{11} \left[1 - \cos \left(\pi \frac{\eta}{\chi_1} \right) \right], \end{aligned}$$

- for the lower part ($0 \leq \eta \leq \chi_2$):

$$(2.2) \quad \begin{aligned} b^{(2)}(\eta) &= b_0 \bar{b}^{(2)}(\eta), \\ \bar{b}^{(2)}(\eta) &= 1 + \frac{1}{2} \beta_{22} \left[1 - \cos \left(\pi \frac{\eta}{\chi_2} \right) \right], \end{aligned}$$

where $\eta = y/h$ – the dimensionless coordinate, $\chi_1 = h_1/h$, and $\chi_2 = h_2/h$ – the dimensionless depths of the upper and lower parts, respectively, $\beta_{10} = b_1/b_0$, $\beta_{20} = b_2/b_0$, $\beta_{11} = \beta_{10} - 1$, $\beta_{22} = \beta_{20} - 1$ – the dimensionless coefficients of the width, moreover $\chi_1 + \chi_2 = 1$.

Based on the zeroing condition of the first moment of this beam cross section about the neutral axis z , one obtains the dimensionless depth of the lower part:

$$(2.3) \quad \chi_2 = \left\{ 1 + \sqrt{\frac{\pi^2 - 4 + (\pi^2 + 4) \beta_{20}}{\pi^2 - 4 + (\pi^2 + 4) \beta_{10}}} \right\}^{-1},$$

and consequently, the dimensionless depth of the upper part $\chi_1 = 1 - \chi_2$.

The deformation of a plane cross section after bending of the beam is shown in Fig. 3.

The longitudinal displacements, according to Fig. 3, are as follows:

- for the upper part ($-\chi_1 \leq \eta \leq 0$):

$$(2.4) \quad u^{(1)}(x, \eta) = -h \left[\eta \frac{dv}{dx} - f_d^{(1)}(\eta) \psi(x) \right],$$

- for the lower part ($0 \leq \eta \leq \chi_2$):

$$(2.5) \quad u^{(2)}(x, \eta) = -h \left[\eta \frac{dv}{dx} - f_d^{(2)}(\eta) \psi(x) \right],$$

where $v(x)$ – the deflection of the beam, $f_d^{(1)}(\eta)$ and $f_d^{(2)}(\eta)$ – the dimensionless deformation functions, $\psi(x) = u(x)/h$ – the dimensionless displacement function, and $u_1(x) = f_d^{(1)}(-\chi_1) u(x)$, $u_2(x) = f_d^{(2)}(\chi_2) u(x)$ – the longitudinal displacements on the upper and lower surfaces of the beam.

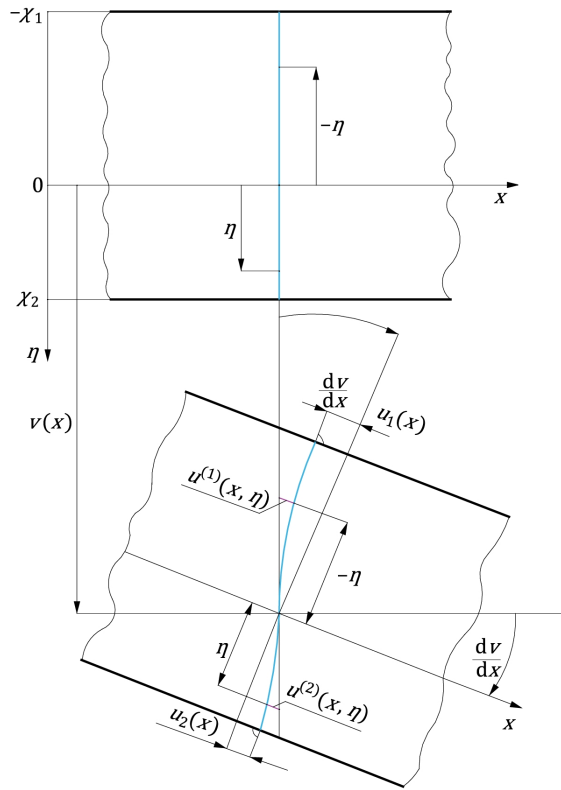


FIG. 3. Scheme of the deformation of a plane cross section of the beam.

Therefore, the strains are in the form:

- for the upper part ($-\chi_1 \leq \eta \leq 0$):

$$\varepsilon_x^{(1)}(x, \eta) = -h \left[\eta \frac{d^2 v}{dx^2} - f_d^{(1)}(\eta) \frac{d\psi}{dx} \right], \quad (2.6)$$

$$\gamma_{xy}^{(1)}(x, \eta) = \frac{df_d^{(1)}}{d\eta} \psi(x),$$

- for the lower part ($0 \leq \eta \leq \chi_2$):

$$\varepsilon_x^{(2)}(x, \eta) = -h \left[\eta \frac{d^2 v}{dx^2} - f_d^{(2)}(\eta) \frac{d\psi}{dx} \right], \quad (2.7)$$

$$\gamma_{xy}^{(2)}(x, \eta) = \frac{df_d^{(2)}}{d\eta} \psi(x).$$

Thus, the normal and shear stresses according to Hooke's law are as follows:

- for the upper part ($-\chi_1 \leq \eta \leq 0$)

$$\sigma_x^{(1)}(x, \eta) = -Eh \left[\eta \frac{d^2v}{dx^2} - f_d^{(1)}(\eta) \frac{d\psi}{dx} \right], \tag{2.8}$$

$$\tau_{xy}^{(1)}(x, \eta) = \frac{E}{2(1+\nu)} \frac{df_d^{(1)}}{d\eta} \psi(x),$$

- for the lower part ($0 \leq \eta \leq \chi_2$)

$$\sigma_x^{(2)}(x, \eta) = -Eh \left[\eta \frac{d^2v}{dx^2} - f_d^{(2)}(\eta) \frac{d\psi}{dx} \right], \tag{2.9}$$

$$\tau_{xy}^{(2)}(x, \eta) = \frac{E}{2(1+\nu)} \frac{df_d^{(2)}}{d\eta} \psi(x),$$

where E – Young's modulus, ν – Poisson's ratio.

The classical shear stress formula called the Zhuravsky shear stress is in the form:

$$\tau_{xy}^{(Cl)}(x, y) = \frac{S_z(y) T(x)}{b(y) J_z}, \tag{2.10}$$

where $T(x)$ – the shear force, and J_z – the second moment of the cross section about the neutral axis defined as:

$$J_z = \int_A y^2 dA = b_0 h^3 \bar{J}_z, \tag{2.11}$$

where the dimensionless second moment is expressed as:

$$\bar{J}_z = \int_{-\chi_1}^0 \eta^2 \bar{b}^{(1)}(\eta) d\eta + \int_0^{\chi_2} \eta^2 \bar{b}^{(2)}(\eta) d\eta. \tag{2.12}$$

The first moment $S_z(y)$ of the cross-sectional area part about the neutral axis is as follows:

- for the upper part ($-\chi_1 \leq \eta \leq 0$):

the first moment of this shaded area is as follows:

$$S_z^{(1)}(\eta) = -b_0 h^2 \bar{S}_z^{(1)}(\eta), \tag{2.13}$$

where the dimensionless first moment is defined as:

$$\bar{S}_z^{(1)}(\eta) = \int_{-\chi_1}^{-\eta} \eta_1 \bar{b}^{(1)}(\eta_1) d\eta_1. \tag{2.14}$$

Figure 4 illustrates the selected area of the beam cross section for the upper part.

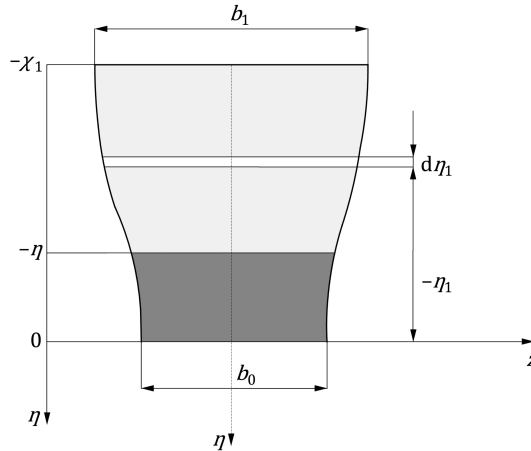


FIG. 4. The selected area of the beam cross section.

Then, after integration, with consideration of the expression (2.1)₂ for dimensionless width, one obtains

$$(2.15) \quad \bar{S}_z^{(1)}(\eta) = \frac{1}{4\pi^2} \left[2\Phi_{11}^{(1)}(\eta) - \Phi_{12}^{(1)}(\eta) \right],$$

where

$$\Phi_{11}^{(1)}(\eta) = \chi_1 (\beta_{10} - 1) \left[\chi_1 \cos\left(\pi \frac{\eta}{\chi_1}\right) + \pi \eta \sin\left(\pi \frac{\eta}{\chi_1}\right) \right],$$

$$\Phi_{12}^{(1)}(\eta) = \beta_{10} \left[\pi^2 \eta^2 - (\pi^2 + 2) \chi_1^2 \right] + \pi^2 \eta^2 - (\pi^2 - 2) \chi_1^2.$$

The dimensionless first moment, for $\eta = 0$, is as follows:

$$(2.16) \quad \bar{S}_z^{(1)}(0) = \bar{S}_{z0}^{(1)} = \frac{\chi_1^2}{4\pi^2} \left[\pi^2 - 4 + (\pi^2 + 4) \beta_{10} \right];$$

- for the lower part ($0 \leq \eta \leq \chi_2$):
the first moment of this shaded area is as follows:

$$(2.17) \quad S_z^{(2)}(\eta) = \left[\bar{S}_{z0}^{(1)} - \int_0^\eta \eta_1 \bar{b}^{(2)}(\eta_1) d\eta_1 \right] b_0 h^2.$$

Then, after integration, with consideration of the expression (2.2)₂ for dimensionless width, one obtains:

$$(2.18) \quad \bar{S}_z^{(2)}(\eta) = \frac{1}{4\pi^2} \left[\chi_1^2 \Phi_0^{(1)} + 2\chi_2 (\beta_{20} - 1) \Phi_{11}^{(2)}(\eta) - \Phi_{12}^{(2)}(\eta) \right],$$

where

$$\begin{aligned} \Phi_0^{(1)} &= \pi^2 - 4 + (\pi^2 + 4) \beta_{10}, \\ \Phi_{11}^{(2)}(\eta) &= \chi_2 \cos\left(\pi \frac{\eta}{\chi_2}\right) + \pi \eta \sin\left(\pi \frac{\eta}{\chi_2}\right), \\ \Phi_{12}^{(2)}(\eta) &= \pi^2 (\beta_{20} + 1) \eta^2 + 2 (\beta_{20} - 1) \chi_2^2. \end{aligned}$$

Figure 5 depicts the selected area of the beam for this case.

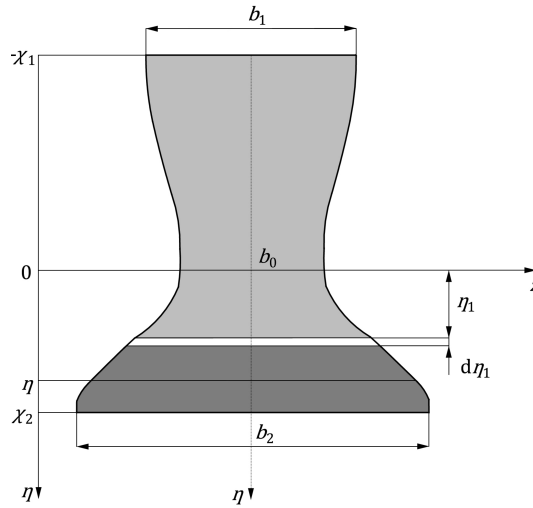


FIG. 5. The selected area of the beam cross section.

It is easy to notice that this first moment, for $\eta = \chi_2$, is equal to zero, i.e., $\overline{S}_z^{(2)}(\chi_2) = 0$.

Equating shear stresses (2.8)₂ and (2.9)₂ to the classical shear stress (2.10) with consideration of the expressions (2.1), (2.13), (2.2), and (2.17), after simple transformation, the unknown dimensionless deformation functions for the upper and lower parts are obtained in the following form:

- for the upper part ($-\chi_1 \leq \eta \leq 0$):

$$(2.19) \quad f_d^{(1)}(\eta) = \int \frac{\overline{S}_z^{(1)}(\eta)}{\overline{b}^{(1)}(\eta)} d\eta,$$

- for the lower part ($0 \leq \eta \leq \chi_2$):

$$(2.20) \quad f_d^{(2)}(\eta) = \int \frac{\overline{S}_z^{(2)}(\eta)}{\overline{b}^{(2)}(\eta)} d\eta.$$

The longitudinal displacements on the upper and lower surfaces of this beam (Fig. 3) are as follows:

$$(2.21) \quad \begin{aligned} u_1(x)/h &= f_d^{(1)}(-\chi_1) \cdot \psi(x), \\ u_2(x)/h &= f_d^{(2)}(\chi_2) \cdot \psi(x). \end{aligned}$$

3. ANALYTICAL FORMULATION AND SOLUTION OF THE BEAM BENDING PROBLEM

The elastic strain energy of this homogeneous beam is as follows:

$$(3.1) \quad U_{es} = Eb_0h \int_0^{L/2} \left\{ \int_{-\chi_1}^0 \Phi_{\varepsilon\gamma}^{(1)}(x, \eta) \bar{b}^{(1)}(\eta) d\eta + \int_0^{\chi_2} \Phi_{\varepsilon\gamma}^{(2)}(x, \eta) \bar{b}^{(2)}(\eta) d\eta \right\} dx,$$

where

$$\begin{aligned} \Phi_{\varepsilon\gamma}^{(1)}(x, \eta) &= \left[\varepsilon_x^{(1)}(x, \eta) \right]^2 + \frac{1}{2(1+\nu)} \left[\gamma_{xy}^{(1)}(x, \eta) \right]^2, \\ \Phi_{\varepsilon\gamma}^{(2)}(x, \eta) &= \left[\varepsilon_x^{(2)}(x, \eta) \right]^2 + \frac{1}{2(1+\nu)} \left[\gamma_{xy}^{(2)}(x, \eta) \right]^2. \end{aligned}$$

Consequently, the above expression (3.1), with consideration of the expressions (2.6) and (2.7) for strains, after integration, is in the form:

$$(3.2) \quad U_{es} = Eb_0h^3 \int_0^{L/2} \left\{ C_{vv} \left(\frac{d^2v}{dx^2} \right)^2 - 2C_{v\psi} \frac{d^2v}{dx^2} \frac{d\psi}{dx} + C_{\psi\psi} \left(\frac{d\psi}{dx} \right)^2 + \frac{C_\psi}{2(1+\nu)} \frac{\psi^2(x)}{h^2} \right\} dx,$$

where

$$\begin{aligned} C_{vv} &= \int_{-\chi_1}^0 \eta^2 \bar{b}^{(1)}(\eta) d\eta + \int_0^{\chi_2} \eta^2 \bar{b}^{(2)}(\eta) d\eta, \\ C_{v\psi} &= \int_{-\chi_1}^0 \eta f_d^{(1)}(\eta) \bar{b}^{(1)}(\eta) d\eta + \int_0^{\chi_2} \eta f_d^{(2)}(\eta) \bar{b}^{(2)}(\eta) d\eta, \\ C_{\psi\psi} &= \int_{-\chi_1}^0 \left[f_d^{(1)}(\eta) \right]^2 \bar{b}^{(1)}(\eta) d\eta + \int_0^{\chi_2} \left[f_d^{(2)}(\eta) \right]^2 \bar{b}^{(2)}(\eta) d\eta, \end{aligned}$$

$$C_\psi = \int_{-x_1}^0 \left(\frac{df_d^{(1)}}{d\eta} \right)^2 \bar{b}^{(1)}(\eta) d\eta + \int_0^{x_2} \left(\frac{df_d^{(2)}}{d\eta} \right)^2 \bar{b}^{(2)}(\eta) d\eta$$

are the dimensionless coefficients.

The work of the load is given by:

$$(3.3) \quad W = 2 \int_0^{L/2} T(x) \frac{dv}{dx} dx,$$

$$\delta W = -2 \int_0^{L/2} \frac{dT}{dx} \delta v dx.$$

Based on the principle of stationary total potential energy $\delta(U_{es} - W) = 0$, the system of two differential equations of equilibrium for this homogeneous beam is obtained in the form:

$$(3.4) \quad C_{vv} \frac{d^4 v}{dx^4} - C_{v\psi} \frac{d^3 \psi}{dx^3} = -\frac{1}{Eb_0 h^3} \frac{dT}{dx},$$

$$(3.5) \quad C_{v\psi} \frac{d^3 v}{dx^3} - C_{\psi\psi} \frac{d^2 \psi}{dx^2} + \frac{C_\psi}{2(1+\nu)} \frac{\psi(x)}{h^2} = 0.$$

Equation (3.4) is equivalent to the equation:

$$(3.6) \quad C_{vv} \frac{d^2 v}{dx^2} - C_{v\psi} \frac{d\psi}{dx} = -\frac{M_b(x)}{Eb_0 h^3},$$

where $M_b(x)$ – the bending moment.

Equations (3.5) and (3.6), after transformation, are reduced to one equation:

$$(3.7) \quad \frac{d^2 \psi}{dx^2} - \alpha^2 \frac{\psi(x)}{h^2} = -\frac{C_{v\psi}}{C_{vv} C_{\psi\psi} - C_{v\psi}^2} \frac{T(x)}{Eb_0 h^3},$$

where

$$\alpha = \sqrt{\frac{1}{2(1+\nu)} \frac{C_{vv} C_\psi}{C_{vv} C_{\psi\psi} - C_{v\psi}^2}}$$

is a dimensionless coefficient.

Equation (3.7) in the dimensionless coordinate $\xi = x/L$ is as follows:

$$(3.8) \quad \frac{d^2 \psi}{d\xi^2} - (\alpha\lambda)^2 \psi(\xi) = -\frac{C_{v\psi}}{C_{vv} C_{\psi\psi} - C_{v\psi}^2} \lambda^2 \frac{T(\xi)}{Eb_0 h},$$

where $\lambda = L/h$ – the relative length of the beam.

The scheme of the reactions force $R = F/2$ and bending moment M_0 in the clamped end of the beam are shown in Fig. 6.

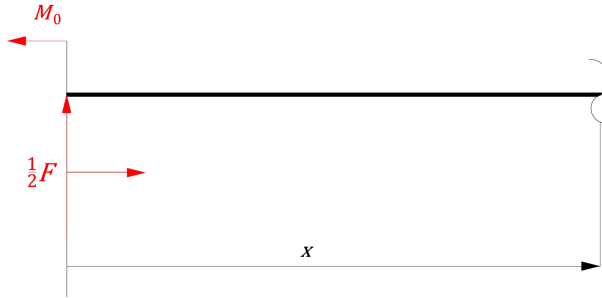


FIG. 6. Scheme of the reactions in clamped end of the beam.

Therefore, the bending moment and shear force, in the dimensionless coordinate ξ ($0 \leq \xi \leq 1/2$), are in the form:

$$(3.9) \quad M_b(\xi) = \left(-\bar{M}_0 + \frac{1}{2}\xi \right) FL, \quad \text{and} \quad T(\xi) = \frac{1}{2}FL,$$

where $\bar{M}_0 = M_0/FL$ – the dimensionless reaction moment.

The solution of Eq. (3.8), considering the shear force $T(\xi) = FL/2$, is in the form:

$$(3.10) \quad \psi(\xi) = \left[C_1 \sinh(\alpha\lambda\xi) + C_2 \cosh(\alpha\lambda\xi) + (1 + \nu) \frac{C_{v\psi}}{C_{vv}C_\psi} \right] \frac{F}{Eb_0h},$$

where C_1, C_2 – integration constants.

These constants, based on the conditions $\psi(0) = 0$ – clamped end, and $\psi(1/2) = 0$ – middle of the beam, are as follows:

$$C_1 = (1 + \nu) \frac{\cosh(\alpha\lambda/2) - 1}{\sinh(\alpha\lambda/2)} \frac{C_{v\psi}}{C_{vv}C_\psi},$$

$$C_2 = -(1 + \nu) \frac{C_{v\psi}}{C_{vv}C_\psi}.$$

Consequently, the dimensionless displacement – the shear effect function – is given in the following form:

$$(3.11) \quad \psi(\xi) = \bar{\psi}(\xi) \frac{F}{Eb_0h},$$

where

- in the first interval $0 \leq \xi \leq 1/2$

$$(3.12) \quad \bar{\psi}(\xi) = \bar{\psi}_1(\xi) \\ = (1 + \nu) \left\{ 1 - \frac{\sinh(\alpha\lambda\xi) + \sinh[(1/2 - \xi)\alpha\lambda]}{\sinh(\alpha\lambda/2)} \right\} \frac{C_{v\psi}}{C_{vv}C_\psi},$$

- in the second interval $1/2 \leq \xi \leq 1$, with the condition $\psi(1) = 0$

$$(3.13) \quad \bar{\psi}(\xi) = \bar{\psi}_2(\xi) \\ = (1 + \nu) \left\{ 1 - \frac{\sinh[(1 - \xi)\alpha\lambda] + \sinh[(\xi - 1/2)\alpha\lambda]}{\sinh(\alpha\lambda/2)} \right\} \frac{C_{v\psi}}{C_{vv}C_\psi}.$$

The shear stress $(2.8)_2$ in the upper part ($-\chi_1 \leq \eta \leq 0$), with consideration of the expressions (3.11), (3.12) and (2.19) is of the form:

$$(3.14) \quad \tau_{xy}^{(1)}(\xi, \eta) = \bar{\tau}_{xy}^{(1)}(\xi, \eta) \frac{F}{b_0h},$$

where the dimensionless shear stress is:

$$(3.15) \quad \bar{\tau}_{xy}^{(1)}(\xi, \eta) = \frac{\bar{S}_z^{(1)}(\eta)}{\bar{b}^{(1)}(\eta)} \left\{ \frac{1}{2} - \frac{\sinh(\alpha\lambda\xi) + \sinh[(1/2 - \xi)\alpha\lambda]}{2 \sinh(\alpha\lambda/2)} \right\} \frac{C_{v\psi}}{C_{vv}C_\psi}.$$

Proceeding similarly to the upper part, the shear stress $(2.9)_2$ in the lower part ($0 \leq \eta \leq \chi_2$) is as follows:

$$(3.16) \quad \tau_{xy}^{(2)}(\xi, \eta) = \bar{\tau}_{xy}^{(2)}(\xi, \eta) \frac{F}{b_0h},$$

where the dimensionless shear stress is:

$$(3.17) \quad \bar{\tau}_{xy}^{(2)}(\xi, \eta) = \frac{\bar{S}_z^{(2)}(\eta)}{\bar{b}^{(2)}(\eta)} \left\{ \frac{1}{2} - \frac{\sinh(\alpha\lambda\xi) + \sinh[(1/2 - \xi)\alpha\lambda]}{2 \sinh(\alpha\lambda/2)} \right\} \frac{C_{v\psi}}{C_{vv}C_\psi}.$$

Equation (3.6) in the dimensionless coordinate ξ ($0 \leq \xi \leq 1/2$), with consideration of the bending moment (3.9), is as follows:

$$(3.18) \quad C_{vv} \frac{d^2\bar{v}}{d\xi^2} = \left[C_{v\psi} \frac{d\bar{\psi}}{d\xi} - \left(\bar{M}_0 - \frac{1}{2}\xi \right) \lambda^2 \right] \frac{F}{Eb_0h},$$

where $\bar{v}(\xi) = v(\xi)/L$ – the relative deflection of the beam.

This equation after integration is of the form:

$$(3.19) \quad C_{vv} \frac{d\bar{v}}{d\xi} = \left[C_3 + C_{v\psi} \bar{\psi}(\xi) - \left(\overline{M}_0 \xi - \frac{1}{4} \xi^2 \right) \lambda^2 \right] \frac{F}{Eb_0 h}.$$

Taking into account the conditions: $d\bar{v}/d\xi|_0 = 0$ and $d\bar{v}/d\xi|_{1/2} = 0$, one obtains the integration constant $C_3 = 0$ and dimensionless reaction moment $\overline{M}_0 = 1/8$.

Integrating this equation and taking into account of the boundary condition $\bar{v}(0) = 0$, one obtains the deflection line of the beam:

$$(3.20) \quad \bar{v}(\xi) = \left[(1 + \nu) f_\psi(\xi) \frac{C_{v\psi}^2}{C_{vv} C_\psi} \frac{1}{\lambda^2} + \frac{1}{8} \left(\frac{1}{2} \xi^2 - \frac{2}{3} \xi^3 \right) \right] \frac{\lambda^2}{C_{vv}} \frac{F}{Eb_0 h},$$

where

$$f_\psi(\xi) = \xi - \frac{\cosh(\alpha\lambda\xi) - 1 + \cosh(\alpha\lambda/2) - \cosh[(1/2 - \xi)\alpha\lambda]}{\alpha\lambda \sinh(\alpha\lambda/2)},$$

the relative maximum deflection (3.20) of the beam is:

$$(3.21) \quad \bar{v}_{\max} = \bar{v}\left(\frac{1}{2}\right) = \widehat{v}_{\max} \frac{F}{Eb_0 h},$$

where the maximum dimensionless deflection is

$$(3.22) \quad \widehat{v}_{\max} = (1 + C_{se}) \frac{\lambda^2}{192 C_{vv}},$$

and the coefficient of shear effect is:

$$(3.23) \quad C_{se} = (1 + \nu) \frac{96}{\lambda^2} \left[1 - 4 \frac{\cosh(\alpha\lambda/2) - 1}{\alpha\lambda \sinh(\alpha\lambda/2)} \right] \frac{C_{v\psi}^2}{C_{vv} C_\psi}.$$

4. EXAMPLE ANALYTICAL STUDIES

The exemplary analytical studies are carried out for bending homogeneous beams with a relative length $\lambda = 20$ and Poisson's ratio $\nu = 0.3$, and with three selected monosymmetric cross sections. The data is specified in Table 1.

Table 1. The values of dimensionless coefficients of widths and depths of selected cross sections.

Cross section	β_{10}	β_{20}	χ_1	χ_2
CS-1	0.5	3.0	0.658191	0.341809
CS-2	1.0	3.0	0.607981	0.392019
CS-3	1.5	3.0	0.571578	0.428422

The graph of dimensionless displacement functions (3.12) and (3.13) in two intervals of the beam with cross section CS-1 is shown in Fig. 7.

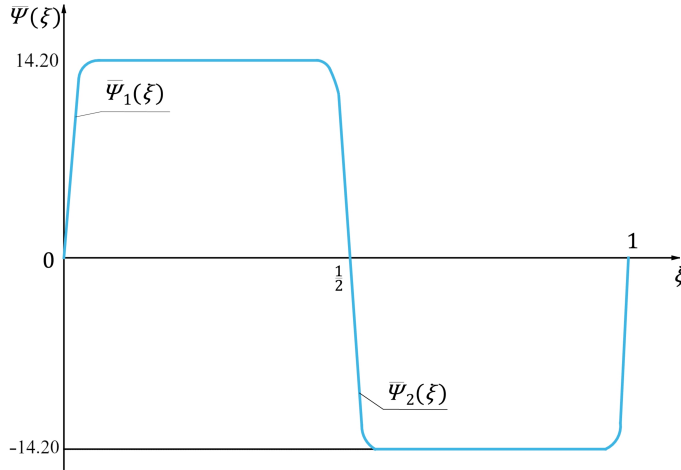


FIG. 7. The graph of dimensionless displacement functions $\bar{\psi}_1(\xi)$ and $\bar{\psi}_2(\xi)$.

The graphs of these functions for the beam with cross sections CS-2 and CS-3 are identical. The extreme values of these functions $\bar{\psi}_{\max} = \bar{\psi}_1(1/4)$ and $\bar{\psi}_{\min} = \bar{\psi}_2(3/4)$ are specified in Table 2.

Table 2. The extreme values of dimensionless displacement functions for selected cross sections.

Cross section	$\bar{\psi}_{\max}$	$\bar{\psi}_{\min}$
CS-1	14.20	-14.20
CS-2	10.21	-10.21
CS-3	8.35	-8.35

The dimensionless shear stress (3.15) of the upper part for $\xi = 1/4$ is as follows:

$$(4.1) \quad \bar{\tau}_{xy}^{(1)}\left(\frac{1}{4}, \eta\right) = \frac{\bar{S}_z^{(1)}(\eta)}{\bar{b}^{(1)}(\eta)} \left\{ \frac{1}{2} - \frac{\sinh(\alpha\lambda/4)}{\sinh(\alpha\lambda/2)} \right\} \frac{C_{v\psi}}{C_{vv}C_\psi},$$

and the dimensionless shear stress (3.17) of the lower part for $\xi = 1/4$ is as follows:

$$(4.2) \quad \bar{\tau}_{xy}^{(2)}\left(\frac{1}{4}, \eta\right) = \frac{\bar{S}_z^{(2)}(\eta)}{\bar{b}^{(2)}(\eta)} \left\{ \frac{1}{2} - \frac{\sinh(\alpha\lambda/4)}{\sinh(\alpha\lambda/2)} \right\} \frac{C_{v\psi}}{C_{vv}C_\psi},$$

Thus, the maximum of these stresses, for $\eta = 0$, is:

$$(4.3) \quad \bar{\tau}_{\max} = \bar{\tau}_{xy}^{(1)} \left(\frac{1}{4}, 0 \right) = \bar{\tau}_{xy}^{(2)} \left(\frac{1}{4}, 0 \right) = \bar{S}_{z0}^{(1)} \left\{ \frac{1}{2} - \frac{\sinh(\alpha\lambda/4)}{\sinh(\alpha\lambda/2)} \right\} \frac{C_{v\psi}}{C_{vv}C_{\psi}}.$$

The values of the shear coefficient C_{se} (3.23), the maximum dimensionless deflection \widehat{v}_{\max} (3.22) and the maximum of the dimensionless shear stresses $\bar{\tau}_{\max}$ (4.3) for the beam with selected cross sections are specified in Table 3.

Table 3. The dimensionless values of the shear coefficient C_{se} , the maximum deflection \widehat{v}_{\max} and maximum shear stresses $\bar{\tau}_{\max}$ for selected cross sections.

Cross section	C_{se}	\widehat{v}_{\max}	$\bar{\tau}_{\max}$
CS-1	0.0332187	23.511	0.767347
CS-2	0.0400257	17.023	0.726022
CS-3	0.0446008	13.984	0.709205

Three selected monosymmetric cross sections and graphs of the dimensionless shear stresses (4.1) and (4.2) for $\xi = 1/4$ in these cross sections of the beam are shown in Fig. 8.

Additionally, example analytical bending studies are carried out for the same beams, but half as long, with relative lengths $\lambda = 10$. The results of these calculations (values: $\bar{\psi}_{\max}$, $\bar{\psi}_{\min}$, $\bar{\tau}_{\max}$) are the same as for beams with relative lengths $\lambda = 20$, while the values of the shear coefficient C_{se} and the maximum deflection \widehat{v}_{\max} are different. The calculation results for the additional case are specified in the Table 4.

Table 4. The dimensionless values of the shear coefficient C_{se} and the maximum deflection \widehat{v}_{\max} for selected cross sections.

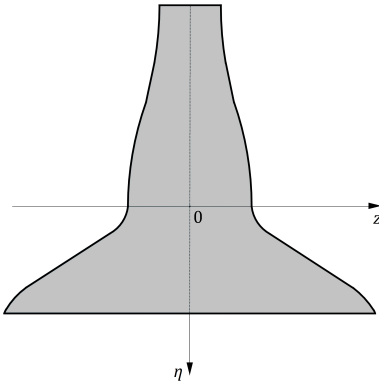
Cross section	C_{se}	\widehat{v}_{\max}
CS-1	0.129682	6.426
CS-2	0.156317	4.732
CS-3	0.174383	3.930

Thus, this nonlinear shear deformation theory can be used in modeling short beams.

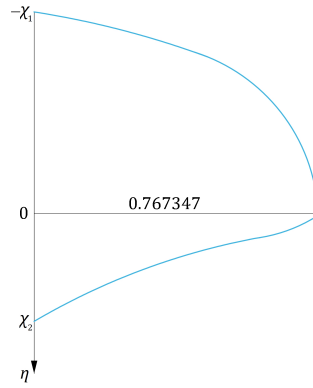
5. NUMERICAL FEM BENDING STUDY OF THE BEAM

In order to validate the analytical model, a numerical analysis was conducted using the finite element method (FEM) in the ABAQUS 2022 environment.

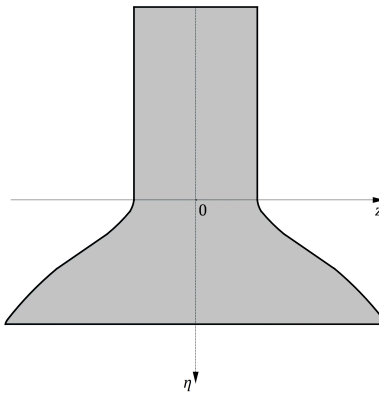
CS-1



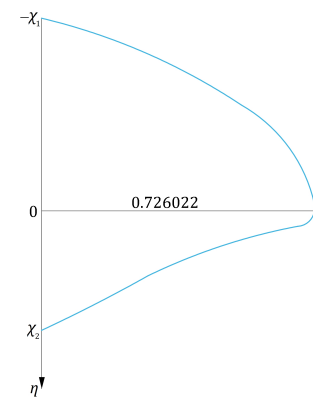
$$\bar{\tau}_{xy}^{(1)}(1/4, \eta) \wedge \bar{\tau}_{xy}^{(2)}(1/4, \eta)$$



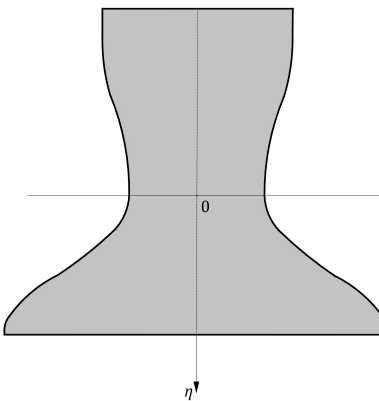
CS-2



$$\bar{\tau}_{xy}^{(1)}(1/4, \eta) \wedge \bar{\tau}_{xy}^{(2)}(1/4, \eta)$$



CS-3



$$\bar{\tau}_{xy}^{(1)}(1/4, \eta) \wedge \bar{\tau}_{xy}^{(2)}(1/4, \eta)$$

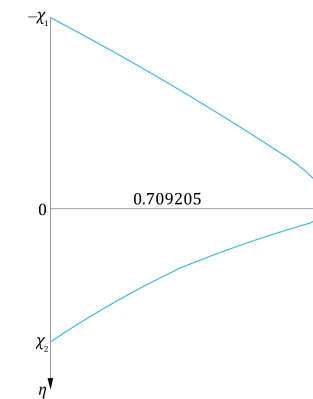


FIG. 8. The beam selected cross sections and graphs of the dimensionless shear stresses.

Numerical models of individual cross sections, namely CS-1, CS-2, and CS-3, with applied boundary conditions, are depicted in Fig. 9. The bending was analyzed only in the xy -plane, according to analytical considerations. The discretization of the beam's model was made with the use of quadratic brick element C3D20R. The convergence of solutions and the size of the problem were considered during preliminary simulations to determine the number of elements along in the depth direction. The distribution of dimensionless shear stresses – results from FEM – is presented in Fig. 10. The validation results of the pre-

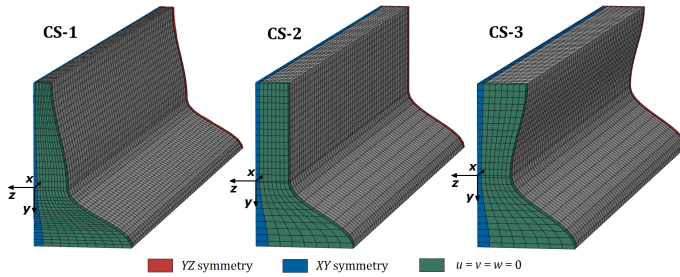


FIG. 9. The numerical models of beams and applied boundary conditions.

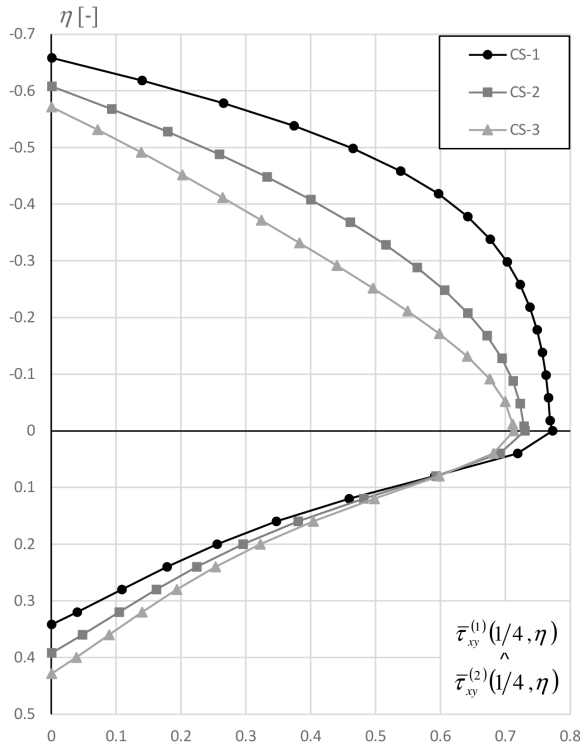


FIG. 10. Distribution of the dimensionless shear stresses – FEM results.

sented analytical model for individual cross sections are shown in Table 5. The percentage relative differences of the analytical and numerical dimensionless deflection \widehat{v}_{\max} range from 0.019% to 0.041%, respectively, and for dimensionless shear stress $\bar{\tau}_{\max}$ from 0.005% to 0.659%, respectively.

Table 5. Comparison of analytical and FEM results.

Cross section		CS-1	CS-2	CS-3
\widehat{v}_{\max}	Analytical	23.511	17.023	13.984
	FEM	23.501	17.019	13.987
	Δ [%]	0.041	0.021	0.019
$\bar{\tau}_{\max}$	Analytical	0.767347	0.726022	0.709205
	FEM	0.772439	0.729466	0.709238
	Δ [%]	0.659	0.472	0.005

6. CONCLUSIONS

In this paper, the problem of three-point bending of a homogeneous clamped beam with a monosymmetric cross section was addressed. A nonlinear shear deformation theory of a plane beam cross section was developed upon which analytical and numerical studies were conducted. Based on the presented analyses, the following conclusions are formulated:

- Analyzing the dimensionless maximum deflections and shear stresses through a comparison of analytical and numerical results reveals a high level of agreement. The maximum relative differences obtained for deflections are definitely below 1‰ and below 1% for shear stresses.
- The distributions of shear stresses were acquired directly on the basis of the nonlinear shear deformation theory with consideration of Zhuravsky shear stress. The planar cross section deformations align closely with the numerical FEM results. This comparative analysis confirms the accuracy of the model, highlighting its capability to account for shear effects that classical beam theories usually neglect.
- The analytical model precisely describes the shear deformation problem of a planar beam cross-section.

REFERENCES

1. WANG C.M., REDDY J.N., LEE K.H., *Shear Deformable Beams and Plates: Relationships with Classical Solutions*, Elsevier, Amsterdam, Lausanne, New York, Oxford, Shannon, Singapore, Tokyo, 2000.

2. KURRER K.-E., *The History of the Theory of Structures: From Arch Analysis to Computational Mechanics*, Ernst & Sohn, Berlin, 2008.
3. REDDY J.N., Nonlocal nonlinear formulations for bending of classical and shear deformation theories of beams and plates, *International Journal of Engineering Science*, **48**(11): 1507–1518, 2010, doi: 10.1016/j.ijengsci.2010.09.020.
4. GAO Y., SHANG L., The exact theory of deep beams without ad hoc assumptions, *Mechanics Research Communication*, **37**(6): 559–564, 2010, doi: 10.1016/j.mechrescom.2010.07.018.
5. CARRERA E., GIUNTA G., PETROLO M., *Beam Structures: Classical and Advanced Theories*, John Wiley & Sons, 2011.
6. CHALLAMEL N., Higher-order shear beam theories and enriched continuum, *Mechanics Research Communication*, **38**(5): 388–392, 2011, doi: 10.1016/j.mechrescom.2011.05.004.
7. THAI H-T., VO T.P., A nonlocal sinusoidal shear deformation beam theory with application to bending, buckling, and vibration of nanobeams, *International Journal of Engineering Science*, **54**: 58–66, 2012, doi: 10.1016/j.ijengsci.2012.01.009.
8. THAI H-T., VO T.P., Bending and free vibration of functionally graded beams using various higher-order shear deformation beam theories, *International Journal of Mechanical Sciences*, **62**(1): 57–66, 2012, doi: 10.1016/j.ijmecsci.2012.05.014.
9. AKGÖZ B., CIVAŁEK Ö., A size-dependent shear deformation beam model based on the strain gradient elasticity theory, *International Journal of Engineering Science*, **70**: 1–14, 2013, doi: 10.1016/j.ijengsci.2013.04.004.
10. REDDY J.N., EL-BORGI S., Eringen's nonlocal theories of beams accounting for moderate rotations, *International Journal of Engineering Science*, **82**: 159–177, 2014, doi: 10.1016/j.ijengsci.2014.05.006.
11. PRADHAN K.K., CHAKRAVERTY S., Effects of different shear deformation theories on free vibration of functionally graded beams, *International Journal of Mechanical Sciences*, **82**: 149–160, 2014, doi: 10.1016/j.ijmecsci.2014.03.014.
12. SENJANOVIĆ I., VLADIMIR N., TOMIĆ M., On new first-order shear deformation plate theories, *Mechanics Research Communication*, **73**: 31–38, 2016, doi: 10.1016/j.mechrescom.2016.02.005.
13. ÖZÜTOK A., MADENCI E., Static analysis of laminated composite beams based on higher-order shear deformation theory by using mixed-type finite element method, *International Journal of Mechanical Sciences*, **130**: 234–243, 2017, doi: 10.1016/j.ijmecsci.2017.06.013.
14. FAGHIDIAN S.A., On non-linear flexure of beams based on non-local elasticity theory, *International Journal of Engineering Science*, **124**: 49–63, 2018, doi: 10.1016/j.ijengsci.2017.12.002.
15. CHALLAMEL N., ELISHAKOFF I., A brief history of first-order shear-deformable beam and plate models, *Mechanics Research Communication*, **102**: 103389, 2019, doi: 10.1016/j.mechrescom.2019.06.005.
16. LIN F., TONG L.H., SHEN H-S., LIM C.W., XIANG Y., Assessment of first and third order shear deformation beam theories for the buckling and vibration analysis of nanobeams incorporating surface stress effects, *International Journal of Mechanical Sciences*, **186**: 105873, 2020, doi: 10.1016/j.ijmecsci.2020.105873.

17. MAGNUCKI K., LEWINSKI J., FAR M., MICHALAK P., Three-point bending of an expanded-tapered sandwich beam – analytical and numerical FEM study, *Mechanics Research Communication*, **103**: 103471, 2020, doi: 10.1016/j.mechrescom.2019.103471.
18. MAGNUCKI K., LEWINSKI J., MAGNUCKA-BLANDZI E., STAWECKA H., Three-point bending of an expanded-tapered beam with consideration of the shear effect, *Journal of Theoretical and Applied Mechanics*, **58**(3): 661–672, 2020, doi: 10.15632/jtam-pl/122203.
19. MAGNUCKI K., PACZOS P., WICHNIAREK R., Three-point bending of beams with consideration of the shear effect, *Steel and Composite Structures, An International Journal*, **37**(6): 733–740, 2020, doi: 10.12989/scs.2020.37.6.733.
20. MALIKAN M., EREMEYEV V.A., A new hyperbolic-polynomial higher-order elasticity theory for mechanics of thick FGM beams with imperfection in the material composition, *Composite Structures*, **249**: 112486, 2020, doi: 10.1016/j.compstruct.2020.112486.
21. MAGNUCKI K., STAWECKI W., MAGNUCKA-BLANDZI E., Bending of beams with consideration of a seventh-order shear deformation theory, *Engineering Transactions*, **68**(2): 119–135, 2020, doi: 10.24423/EngTrans.1129.20200214.
22. MAGNUCKI K., LEWINSKI J., MAGNUCKA-BLANDZI E., A shear deformation theory of beams of bisymmetrical cross-sections based on the Zhuravsky shear stress formula, *Engineering Transactions*, **68**(4): 353–370, 2020, doi: 10.24423/EngTrans.1174.20201120.
23. MAGNUCKI K., LEWINSKI J., MAGNUCKA-BLANDZI E., An improved shear deformation theory for bending beams with symmetrically varying mechanical properties in the depth direction, *Acta Mechanica*, **231**(10): 4381–4395, 2020, doi: 10.1007/s00707-020-02763-y.
24. MAGNUCKI K., An individual shear deformation theory of beams with consideration of the Zhuravsky shear stress formula, [in:] *Current Perspectives and New Directions in Mechanics, Modelling and Design of Structural Systems*, Zingoni A. [Ed.], CRC Press, Taylor & Francis Group, Boca Raton, London, New York, 2022, doi: 10.1201/9781003348443-112.

Received January 31, 2024; accepted version May 23, 2024.

Online first July 9, 2024.



Copyright © 2024 The Author(s).
Published by IPPT PAN. This work is licensed under the Creative Commons Attribution License
CC BY 4.0 (<https://creativecommons.org/licenses/by/4.0/>).